

Propagation Instabilities of High-Intensity Laser-Produced Electron Beams

M. Tatarakis,^{1,2} F. N. Beg,¹ E. L. Clark,³ A. E. Dangor,¹ R. D. Edwards,³ R. G. Evans,³ T. J. Goldsack,³
K. W. D. Ledingham,⁶ P. A. Norreys,⁴ M. A. Sinclair,³ M.-S. Wei,¹ M. Zepf,⁵ and K. Krushelnick¹

¹*The Blackett Laboratory, Imperial College of Science, Technology, and Medicine, London SW7 2BZ, United Kingdom*

²*Institute of Matter Structure and Laser Physics (IMLP), Technical University of Crete, 73100 Chania, Crete, Greece*

³*AWE plc, Aldermaston, Reading, RG7 4PR, United Kingdom*

⁴*Rutherford Appleton Laboratory, Chilton, Didcot, Oxon OX11 0QX, United Kingdom*

⁵*Department of Physics, The Queen's University, Belfast BT7 1NN, United Kingdom*

⁶*Department of Physics, University of Glasgow, Glasgow BT7 1NN, United Kingdom*

(Received 28 November 2002; published 29 April 2003)

Measurements of energetic electron beams generated from ultrahigh intensity laser interactions ($I > 10^{19}$ W/cm²) with dense plasmas are discussed. These interactions have been shown to produce very directional beams, although with a broad energy spectrum. In the regime where the beam density approaches the density of the background plasma, we show that these beams are unstable to filamentation and “hosing” instabilities. Particle-in-cell simulations also indicate the development of such instabilities. This is a regime of particular interest for inertial confinement fusion applications of these beams (i.e., “fast ignition”).

DOI: 10.1103/PhysRevLett.90.175001

PACS numbers: 52.38.Kd, 52.35.Vd

Short pulse laser technology has allowed the development of very high power laser systems over the past several years [1]. This has consequently enabled experiments using laser pulses focused to extreme intensities (up to $I \sim 10^{20}$ W/cm²), thus making possible the exploration of relativistic plasma physics in the laboratory. For example, when such high intensity laser pulses are focused into a plasma, very energetic electrons [2], ions [3], and gamma rays [4] can be observed.

One of the most exciting applications for these exotic laser-produced plasmas is in the context of fast ignition [5,6] for inertial confinement fusion (ICF). In this scheme, a high power laser generates a short pulse, high current electron beam [7] at the edge of a cold, highly compressed plasma of deuterium and tritium (DT). This electron beam is then used to spark a burn wave able to propagate throughout the fuel—consequently generating fusion energy. The resulting separation of compression and heating stages in ICF may be able to reduce greatly the total energy and symmetry requirements for the compression. Much of the physics involved in the realization of this scheme is the subject of current research. Indeed, there are questions as to the conversion efficiency of high intensity laser light into fast electrons, the propagation of such high current relativistic electron beams through dense plasma and the energy deposition characteristics of these beams.

In this Letter, we discuss recent experiments carried out to measure the properties of these electron beams. In particular, since current laser systems are unable to generate electron beams with sufficient current density to be useful for fast ignition—we study the propagation of electron beams produced by present state-of-the-art laser systems in lower density plasma. Since the ratio of the

beam density to background plasma density may be similar for our experiments to that envisaged for full fast ignition experiments (while the beam “temperature” and emittance are also similar) the characteristics of electron beam propagation may be comparable.

To show the relevance of our experiments to fast ignition it is possible to estimate the parameters of the electron beam required to heat a region of plasma to ignition (i.e., an areal density $\rho r = 0.3$ g cm⁻² and temperature ~ 10 keV, where ρ is the compressed plasma density and r is the radius of the compressed fuel). For $\rho = 300$ g cm⁻³, one requires ~ 10 kJ of hot electron energy with $E_{\text{average}} = 1.5$ MeV, implying a beam containing 4×10^{16} electrons (assuming that 10% of the electron energy is deposited). If the radius of the hot spot is 10 μ m, a beam density of $n_b \sim 3 \times 10^{23}$ cm⁻³ for the case of a 1 ps pulse is implied. This consequently corresponds to the electron density in a 3 g/cm³ DT plasma. However, electron beams of the required density have never been previously produced.

The electron beams currently produced in high intensity laser plasma interaction experiments are significantly below this level although they do have currents greater than the limiting current for vacuum propagation (i.e., the Alfvén current: $I_A = 1.7 \times 10^4 \beta \gamma = 54$ kA for $\gamma = 3$). Previous experiments suggest that $\sim 10^{13-14}$ hot electrons can be produced (up to 50% conversion efficiency) and the hot electron temperature was measured to be around 1.5–2 MeV [4] for interactions at $I \sim 2 \times 10^{19}$ W/cm². The electron current in present experiments is therefore 10–50 times I_A and the electron beam density is $\sim 10^{20}$ cm⁻³. But this is significantly lower than the beam current required for actual fast ignition experiments ($\sim 10^4 I_A$). Electron beams greater than the Alfvén current can

propagate only in a plasma if they are almost perfectly compensated by a cold return current produced by the background electrons.

In previous solid target interaction experiments, the forward current density was several orders of magnitude less than the target electron plasma density and could easily be compensated [8]. However, as the electron beam density increases and approaches the background electron density, stable propagation is consequently more difficult. Therefore, we have carried out a series of experiments to investigate fast ignition by allowing the beam generated from a relativistic laser interaction with a solid target to propagate from the solid target into a gas (low density plasma). The electron beam density is then comparable to the background electron density in the gaseous plasma. The beam-plasma interaction is also easier to diagnose in these lower density plasmas.

These experiments were carried out using the high power VULCAN Nd:glass laser system. The laser has a wavelength of $1.054 \mu\text{m}$, a pulse length of 0.9–1.2 psec and a pulse energy of 50–70 J. The laser beam was focused onto the target surface using a 60 cm focal length off-axis parabolic mirror. The laser beam was *p*-polarized and was incident at an angle of 45° . The peak intensity was found to be about $5 \times 10^{19} \text{ W/cm}^2$ using simultaneous measurements of the laser parameters. The targets were typically thin foils (50–175 μm) of aluminum or Mylar (CH). Mylar targets were coated with 0.1–1 μm of aluminum.

In this experiment, a gas jet was placed immediately behind the target (see Fig. 1). The gas/plasma was probed transversely using shadowgraphy and Moiré deflectometry with a picosecond duration ($\lambda = 527 \text{ nm}$) diagnostic beam to observe plasma density gradients associated with the propagation of the laser-produced electron beam. The supersonic gas jet produced a high density region of gas (up to a maximum of $\sim 5 \times 10^{20} \text{ atoms/cm}^3$) of either helium or argon. From previous measurements the electron density in the plasmas used in these experiments was estimated to be $10^{20} \text{ electrons/cm}^3$ in the case of helium and $10^{21} \text{ electrons/cm}^3$ in argon.

Electrons in the gas are initially in atomic bound states and are quickly ionized during the interaction. This process can be observed in Fig. 2 which shows two shadowgraphs of the ionization process. These were taken synchronously with the interaction of the main laser beam at the front of the target. The observed filaments are due to collisional ionization and/or field ionization of the gas by diverging lower energy electron beams produced during the initial phase of the intense laser interaction (by the leading edge of the laser) and which are uncollimated. This is likely similar to the mechanism of ionization of the interior of the solid target [8]. Note that it is not possible for the laser radiation to propagate through these targets since they were more than 50 μm thick. Consequently, the structures observed in the underdense plasma must be due to the propagation of the laser-

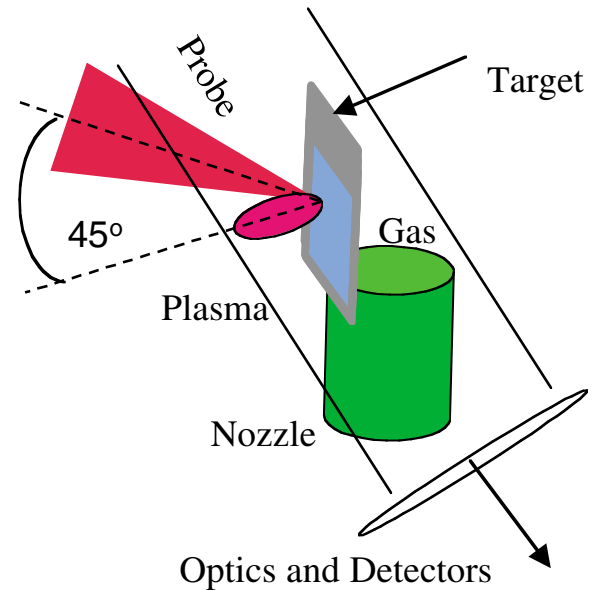


FIG. 1 (color). Experimental setup for gas jet probing experiments.

produced electrons. The origin of the ionization filaments seems to be the interaction region at the front surface of the target. In contrast, x-ray photoionization would not produce the observed filamentary structure since the majority of x rays generated by electron bremsstrahlung are low energy ($< 1 \text{ MeV}$) and are not highly directional. It should also be noted that there was no distortion of the back surface of the target at early times.

In these experiments, it was also possible to make observations of the energy deposition of the main electron beam which exhibits collimation upon leaving the dense solid plasma. After the initial ionization, structures in the gas appear at later times (30–300 ps) which are clearly due to the deposition of energy in the gas by the majority of the laser-generated electrons and which have been collimated into a beam before leaving the solid target. Although the energetic electron beam is generated during the time of the high intensity laser pulse, the propagation path of the beam is visible in the gas only after the heated

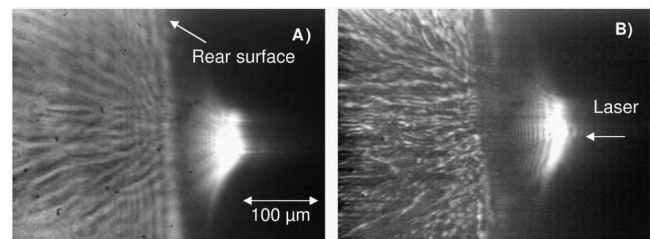


FIG. 2. Shadowgraphy of rear side of solid/gas target during high intensity laser interaction. Probing time is synchronous with main beam interaction and the laser is incident from the right. The bright region is self-generated second harmonic emission (527 nm) at the front surface. Argon was used behind Mylar targets. (a) $I \sim 10^{19} \text{ W/cm}^2$, (b) $I \sim 2 \times 10^{19} \text{ W/cm}^2$.

plasma has time to expand, forming plasma density gradients which can be measured using shadowgraphy. This effect has previously been used to produce plasma density channels in low density gas for use as a high intensity laser waveguide [9].

Figure 3 shows the propagation path of an electron beam exiting a 50 μm Mylar target into a low density helium plasma. The probe image shown is taken at late time (300 ps after the pulse). In this experiment the electron beam remains collimated over about 50 μm upon entering the gas plasma after which it filaments and hoses. Significant shot-to-shot variations of the propagation pattern were also observed; however, filamentation and hosing of the beam in the low density plasma region was a characteristic of all cases studied. This was observed for distances of the order of 100 μm which is about an order of magnitude larger than the electron plasma wavelength. When argon ($n_e \sim 10^{21} \text{ cm}^{-3}$) was used, similar structures were observable (see Fig. 4) but more distinctly and at earlier times. Clearly such structures cannot be the result of energy deposition by radiation or by neutral plasma “jets”—but rather of the beam of electrons produced during the interaction. It should also be noted that no significant proton or ion acceleration was observed at the rear of the target during these experiments so this is unlikely to have contributed to the observed structure. These data were also taken before shock breakout at the rear of the target which occurs several nanoseconds later. Consequently, the observed filamentation in Fig. 3 is likely the result of a Weibel-like instability [10] which is observed after the beam has propagated some distance in the plasma.

The Weibel instability is observed as a filamentation of the electron beam due to variations in the plasma return current and will grow until the filament charge density exceeds that of the return current [11]. The growth rate of the simple Weibel instability is given by

$$\gamma = \omega_{pe} \left[\frac{n_b}{\gamma_b n_e} \right]^{1/2} \frac{v_b}{c},$$

where ω_{pe} is the electron plasma frequency, n_b/n_e is the ratio of the beam density to the background plasma density, v_b is the beam velocity, and γ_b is the relativistic Lorentz factor of the beam. In our experiment the pulse length of the electron beam is likely more than an order of magnitude longer than the inverse plasma frequency. Consequently, this suggests that for relativistic electron beams which have a density comparable to the background plasma density the Weibel instability may become important. However, the initial uncollimated electron cloud (see Fig. 2) is also susceptible to fine-scale filamentation during the electron beam generation process. It is likely that the observed collimated structures on the shadowgrams at later times (Figs. 3 and 4) result from the coalescence of these filaments.

The observed hosing motion of the collimated beam as it propagates in the gas is likely due to the coupling between the Weibel instability with the two-stream instability [12]. This transverse motion is probably not due to the conventional fire-hose instability since this requires that the collision time is short with respect to the e -beam duration (i.e., that the conductivity is low) which is not the case here. From our experiments, it appears that significant hosing as well as “pinching” can occur either before or after beam breakup.

We estimate from the channel expansion rate that the plasma has been heated to ~ 100 eV. The expansion rate is relatively uniform throughout the underdense plasma indicating that the energy loss of the electron beam into the gas over the characteristic distances in this experiment is small compared to the total energy in the beam. It is likely, however, because of the low energy deposition rate observed and the reasonable uniformity of the observed heated region, that collisional processes were the principal cause of the observed heating of the background gas by the electron beam exiting the solid target—although energy can also be lost through the generation of Langmuir turbulence.

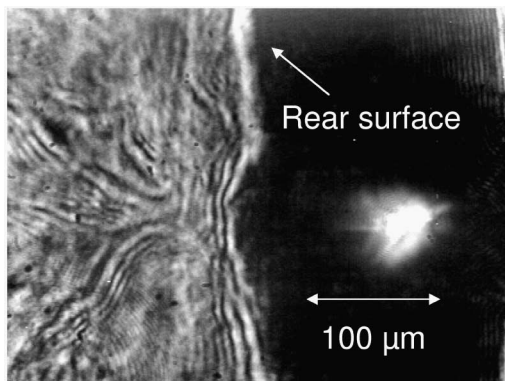


FIG. 3. Shadowgraph at later times in helium (300 ps after the main interaction). $I_{\text{laser}} \sim 2 \times 10^{19} \text{ W/cm}^2$. Target is 50 μm thick Mylar.

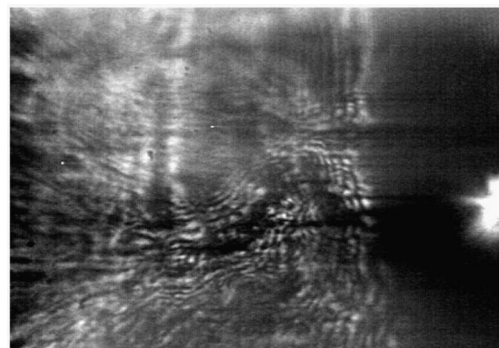


FIG. 4. Shadowgraph in argon (120 ps after the main interaction). $I_{\text{laser}} \sim 2 \times 10^{19} \text{ W/cm}^2$. Target is 50 μm Mylar.

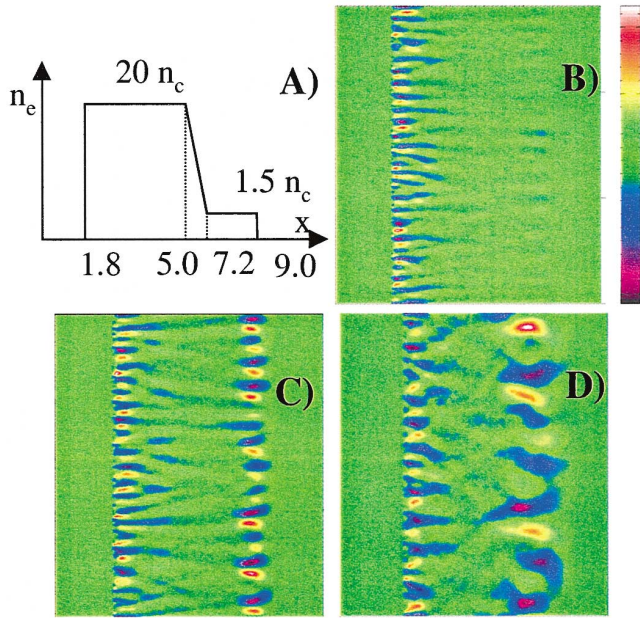


FIG. 5 (color). The dc magnetic fields resulting from 2D OSIRIS particle-in-cell simulation. Initial conditions were the propagation of a plane $1 \mu\text{m}$ wavelength laser beam ($I = 10^{19} \text{ W cm}^{-2}$) from the left onto a plasma with density profile shown in (a) (units in μm). The fields resulting from the filamentation, bending, and coalescence of the laser generated electron beams are shown at (b) 48 fsec, (c) 72 fsec, and (d) 144 fsec after the beginning of the laser pulse (scale varies between $\pm 55 \text{ MG}$).

In order to understand these effects better we have performed 2D simulations of electron beam propagation using the particle-in-cell (PIC) code OSIRIS [13] in which a plane electromagnetic wave at an intensity of $I \sim 10^{19} \text{ W/cm}^2$ (top-hat temporal profile with a rise time of 10 fsec) interacted with a collisionless high density plasma ($20n_{cr}$) which has a low density region at the rear surface as in the experiment. Figure 5 displays three “snapshots” of the magnetic field structure produced by the laser-generated electron beam at different times during the interaction. It is clear that at early times in the laser pulse the structure of the electron beam at the rear surface is composed of fine-scale filaments (of size $\sim c/\omega_{pe}$) which is similar to the component of the electron beam which produces ionization of the gas at the rear of the target as observed in the experiment. Subsequently the electron beam undergoes a considerable amount of coalescence at the rear of the target which likely corresponds to the large scale structures observed in the underdense gas produced at later times in the experiment. In the experiment this gives rise to a “map” of where electron beam energy was deposited in the plasma. From the simulations there is clearly a coupling between the Weibel and the two-stream instability (i.e., bending of filaments is observable). These simulations qualitatively agree with the shadowgraphy measurements and suggest

that both filamentation and the two-stream instability may be significantly enhanced in the low density region of plasma in the experiment.

Therefore in this experiment it is likely that the front of the electron beam undergoes fine-scale filamentation due to the Weibel instability and which can be observed in the ionization structures in the gas at the rear of the target. This instability grows such that the filaments are observed to coalesce into a single collimated beam as it propagates through the solid target and exits the rear surface. As this beam subsequently propagates through the low density plasma it can be subject to severe filamentation and the two-stream instability resulting in the observed hosing.

In conclusion, we have used an innovative target design to perform the first studies of the propagation of very high current laser-produced electron beams in a regime relevant to the fast ignition scheme. Although it appears that such beams can be subject to both the filamentation (Weibel) and two-stream instabilities in plasmas where the beam density is close to the background plasma density—use of cone-guided schemes for fast ignition [6] may be able to reduce the propagation distance of the electron beam and reduce the effect of these instabilities.

The authors acknowledge the assistance of the staff of the Central Laser Facility of the Rutherford Appleton Laboratory as well as the support of the UK EPSRC and the EU for the Marie Curie ERB 5004-CT98-5010 and FU05-CT-2002-50501 projects. We gratefully acknowledge the OSIRIS consortium consisting of UCLA/IST(Portugal)/USC for the use of OSIRIS.

-
- [1] M. D. Perry and G. Mourou, *Science* **264**, 917 (1994).
 - [2] E. Esarey *et al.*, *IEEE Trans. Plasma Sci.* **24**, 252 (1996); M. I. K. Santala *et al.*, *Phys. Rev. Lett.* **86**, 1227 (2001).
 - [3] E. L. Clark *et al.*, *Phys. Rev. Lett.* **85**, 1654 (2000); R. A. Snavely *et al.*, *Phys. Rev. Lett.* **85**, 2945 (2000); E. L. Clark *et al.*, *Phys. Rev. Lett.* **84**, 670 (2000).
 - [4] M. H. Key *et al.*, *Phys. Plasmas* **5**, 1966 (1998); M. I. K. Santala *et al.*, *Phys. Rev. Lett.* **84**, 1459 (2000).
 - [5] M. Tabak *et al.*, *Phys. Plasmas* **1**, 1626 (1994).
 - [6] R. Kodama *et al.*, *Nature (London)* **412**, 798 (2001).
 - [7] S. C. Wilks *et al.*, *Phys. Rev. Lett.* **69**, 1383 (1992).
 - [8] E. Fill, *Phys. Plasmas* **8**, 4613 (2001); M. Tatarakis *et al.*, *Phys. Rev. Lett.* **81**, 999 (1998); M. Borghesi *et al.*, *Phys. Rev. Lett.* **83**, 4309 (1999); L. Gremillet *et al.*, *Phys. Rev. Lett.* **83**, 5015 (1999).
 - [9] C. G. Durfee and H. M. Milchberg, *Phys. Rev. Lett.* **71**, 2409 (1993).
 - [10] E. S. Weibel, *Phys. Rev. Lett.* **2**, 83 (1959).
 - [11] M. Honda *et al.*, *Phys. Rev. Lett.* **85**, 2128 (2000); L. O. Silva *et al.*, *Phys. Plasmas* **9**, 2458 (2002); L. Gremillet *et al.*, *Phys. Plasmas* **9**, 941 (2002).
 - [12] E. S. Dodd *et al.*, *Phys. Rev. Lett.* **88**, 125001 (2002).
 - [13] R. Hemker, Ph.D. dissertation, UCLA, 2000.